Amino Acids (2013) 45:143–157
DOI 10.1007/s00726-013-1482-4

ORIGINAL ARTICLE

Panurgines, novel antimicrobial peptides from the venom of communal bee *Panurgus calcaratus* (Hymenoptera: Andrenidae)

Sabína Čujová · Jiřina Slaninová · Lenka Monincová · Vladimír Fučík · Lucie Bednárová · Jitka Štokrová · Oldřich Hovorka · Zdeněk Voburka · Jakub Straka · Václav Čeřovský

Received: 16 November 2012 / Accepted: 23 February 2013 / Published online: 13 March 2013

Abstract Three novel antimicrobial peptides (AMPs), named panurgines (PNGs), were isolated from the venom of the wild bee *Panurgus calcaratus*. The dodecapeptide of the sequence LNWGAILKHIIK-NH_2 (PNG-1) belongs to the category of α-helical amphipathic AMPs. The other two cyclic peptides containing 25 amino acid residues and two intramolecular disulfide bridges of the pattern Cys8–Cys23 and Cys11–Cys19 have almost identical sequence established as LDVKKIICVACKIXPNPACKKICPK-OH (X=K, PNG-K and X=R, PNG-R). All three peptides exhibited antimicrobial activity against Gram-positive bacteria and Gram-negative bacteria, antifungal activity, and low hemolytic activity against human erythrocytes. We prepared a series of PNG-1 analogs to study the effects of cationicity, amphipathicity, and hydrophobicity on the biological activity. Several of them exhibited improved antimicrobial potency, particularly those with increased net positive charge. The linear analogs of PNG-K and PNG-R having all Cys residues substituted by α-amino butyric acid were inactive, thus indicating the importance of disulfide bridges for the antimicrobial activity. However, the linear PNG-K with all four cysteine residues unpaired, exhibited antimicrobial activity. PNG-1 and its analogs induced a significant leakage of fluorescent dye entrapped in bacterial membrane-mimicking large unilamellar vesicles as well as in vesicles mimicking eukaryotic cell membrane. On the other hand, PNG-K and PNG-R exhibited dye-leakage activity only from vesicles mimicking bacterial cell membrane.

Keywords Antimicrobial peptides · Wild bee venom · CD spectroscopy · Large unilamellar vesicles · Electron microscopy

Introduction

Antimicrobial peptides (AMPs) have been identified in almost all forms of life as important components of the innate immune systems. Most of these have positive net charge, consist of 10–50 amino acid residues, and exhibit amphipathic structure upon interaction with biological membrane or a membrane-mimicking environment. These features enable them to interact with bacterial cell membrane and disrupt it by several different mechanisms that have lethal impact on bacteria. Some AMPs may penetrate through the cell membrane and hit the key intracellular targets or interfere with bacteria metabolism (Amiche and Galanth 2011; Brandenburg et al. 2012; Epand and Epand 2011; Huang et al. 2010; Toke 2005; Teixeira et al. 2012; Wimley and Hristova 2011; Yeaman and Yount 2003). Due to their unique mechanisms of action that differ from those

Electronic supplementary material The online version of this article (doi:10.1007/s00726-013-1482-4) contains supplementary material, which is available to authorized users.

S. Čujová · J. Slaninová · L. Monincová · V. Fučík · L. Bednárová · J. Štokrová · O. Hovorka · Z. Voburka · V. Čeřovský (✉)
Institute of Organic Chemistry and Biochemistry, Academy of Sciences of the Czech Republic, Flemingovo nám. 2, 16610 Prague 6, Czech Republic
e-mail: cerovsky@uochb.cas.cz

S. Čujová · L. Monincová
Department of Biochemistry, Faculty of Science, Charles University in Prague, Hlavova 8, 12843 Prague 2, Czech Republic

J. Straka
Department of Zoology, Faculty of Science, Charles University in Prague, Viničná 7, 12843 Prague 2, Czech Republic

of conventional antibiotics, interest has grown in AMPs as new drug candidates with potential to overcome the bacterial resistance to antibiotics (Baltzer and Brown 2011; Brandenburg et al. 2012; Giuliani et al. 2007; Oyston et al. 2009; Yeung et al. 2011; Zaiou 2007).

Among more than 1,000 AMPs listed in the Antimicrobial Peptide Database (Wang et al. 2009), those peptides found in the venom of stinging Hymenoptera such as honeybees, wasps, bumblebees and ants comprise a group of pharmacological interest (Kuhn-Nentwig 2003). Most of these belong to the class of cationic peptides with amphipathic α-helical conformation (Tossi et al. 2000). For example, melittin (Asthana et al. 2004) isolated from the venom of honeybees; mastoparans (Čeřovský et al. 2008a), anoplin (Konno et al. 2001), eumenitin (Konno et al. 2006), and decoralin (Konno et al. 2007) isolated from the venom of wasps; bombolitins (Argiolas and Pisano 1985) from bumblebee venom are cytolytic peptides possessing potent antimicrobial activity against a broad range of bacteria. In the course of our continuing survey of new AMPs, we have found that the venom of wild bees represents another source of promising peptides showing potent antimicrobial activity and low or moderate hemolytic activity. Those are melectin (Čeřovský et al. 2008b), lasioglossins (Čeřovský et al. 2009), halictines (Monincová et al. 2010), and macropin (Monincová et al. 2009), which are linear peptides of the α-helical category consisting of 12–18 amino acid residues. In the venom of *Lasioglossum laticeps*, in addition to the aforementioned α-helical lasioglossins, we identified lasiocepsin, a peptide containing 27 amino acid residues and two disulfide bridges (Monincová et al. 2012).

An intrinsic distinction in composition between bacterial and eukaryotic membranes provides a basis for the preference of cationic AMPs to act in relation to bacterial membranes. The prevalent negative net charge of bacterial membranes due to the composition of their phospholipids (predominantly with negative charge) plays a major role in the attraction of the cationic AMPs, while membranes of eukaryotic cells enriched in zwitterionic phospholipids and cholesterol are refractory to the AMPs.

Studies of AMP interactions with membranes at the molecular level are important for understanding processes of membrane disruption or permeabilization. Model membranes of a composition reflecting those of bacterial or eukaryotic membranes made in the form of liposomes constitute a simple but valuable tool for understanding the principles of peptide–membrane interactions and may help to explain the mechanism of bacterial sensitivity—or of eukaryotic cells insensitivity—to AMPs (Lohner and Blondele 2005; Shailesh et al. 2009; Vemuri and Rhodes 1995).

The present work describes isolation, structural characterization, synthesis, and structural activity relationships of three novel AMPs named panurgines (PNGs) which we identified in the venom of the wild bee *P. calcaratus* (this species inhabits summer communal colonies burrowed in sandy soil and collects pollen from yellow Asteraceae flowers), i.e., one short linear α-helical peptide and two, almost identical cyclic peptides consisting of 25 amino acids residues and two disulfide bridges. One of these analogs was selected for the study of its effect on the morphology of *Bacillus subtilis* by transmission electron microscopy.

In addition, this study focuses on the interactions of PNGs with artificial membranes, which are liposomes constructed from various phospholipids. We investigated interactions of PNGs with negatively charged liposomes composed of 1,2-dioleoyl-*sn*-glycero-3-phosphocholine (DOPC) and 1,2-dipalmitoyl-*sn*-glycero-3-[phospho-rac-1-glycerol] (DPPG) (1:2, mol/mol) or DOPC and 1,2-dioleoyl-*sn*-glycero-3-[phospho-rac-1-glycerol] (DOPG) (1:2, mol/mol) as a general model of bacterial membranes. Liposomes made from 1,2-dioleoyl-*sn*-glycero-3-phosphoethanolamine (DOPE), DOPG, and heart bovine cardiolipin (CL) (15:80:5, mol/mol/mol) were used as a possible model for *B. subtilis* membrane (Epand et al. 2007). Liposomes made solely from uncharged DOPC served as model membranes of erythrocytes.

Materials and methods

Materials

Fmoc-protected L-amino acids, 2-chlorotrityl chloride resin, and Rink Amide MBHA resin were purchased from IRIS Biotech GmbH, Marktredwitz, Germany. Tetracycline, LB broth, LB agar, and thermolysin were obtained from Sigma-Aldrich. All other reagents, solvents, and HPLC-grade acetonitrile were of the highest purity available from commercial sources. Phospholipids were purchased from Avanti Polar Lipids (Alabaster, AL, USA), and fluorescent dye calcein was from Sigma-Aldrich. As test organisms, we used *B. subtilis* (*B.s.*) 168, kindly provided by Prof. Yoshikawa (Princeton University, Princeton, NJ, USA). *Escherichia coli* (*E.c.*) B and *Micrococcus luteus* (*M.l.*) No. CCM 144 were from the Czech Collection of Microorganisms, Brno, Czech Republic; *Staphylococcus aureus* (*S.a.*) and *Pseudomonas aeruginosa* (*P.a.*) were obtained as multiresistant clinical isolates; *Candida albicans* (*C.a.*) (F7-39/IDE99) came from the mycological collection of the Faculty of Medicine, Palacky University, Olomouc, Czech Republic.

Sample preparation and peptide purification

Bee specimens of *P. calcaratus* were collected in the area of the city of Kladno in the Czech Republic during August 2010 and were then kept frozen at −20 °C. The

venom reservoirs of eight individuals were dissected under a microscope and their contents extracted using a mixture of acetonitrile and water (1:1) containing 0.5 % trifluoroacetic acid (40 μL). The extract was centrifuged, and the supernatant was fractionated by RP-HPLC. Chromatography was carried out on an Agilent Technologies 1200 Series module with a Vydac C-18 (250 × 4.6 mm; 5 μm) column, (Grace Vydac, Hesperia, CA, USA) at a 1-mL/min flow rate using a solvent gradient ranging from 5 to 70 % acetonitrile/water/0.1 % TFA over 60 min (Fig. 1). The elution was monitored by absorption at 220, 254 and 280 nm utilizing a diode-array detector. The instrument was controlled and the UV spectra evaluated using ChemStation Software. The selected fractions (peaks detected at 220 nm) were manually collected, the solvent evaporated in a Speed-Vac, and the material tested for antimicrobial activity against *M. luteus* by drop diffusion assay. The active fractions were further analyzed by mass spectrometry and subjected to Edman degradation.

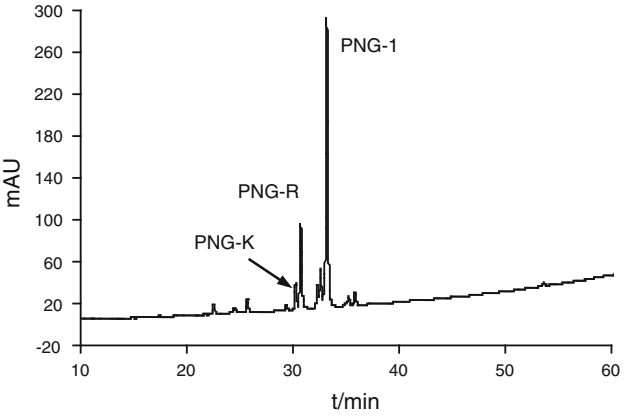

Fig. 1 RP-HPLC profile of *Panurgus calcaratus* venom extract at 220 nm. An elution gradient of solvents from 5 to 70 % acetonitrile/water/0.1 % TFA was applied for 60 min at flow rate 1 mL/min

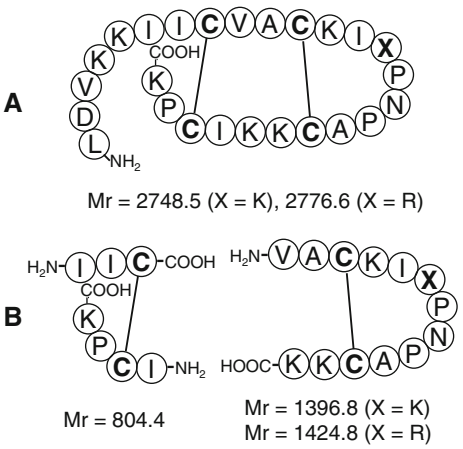

Fig. 2 Primary structures of PNG-K and PNG-R (**a**) and determination of their disulfide bridges patterns as Cys8–Cys23 and Cys11–Cys19 (**b**). Two peptide fragments (**b**) resulting from the digestion of PNG-K(R) by thermolysin were isolated by RP-HPLC and their mass determined by ESI–MS. Mr values denote calculated molecular masses (monoisotopic) of peptides that were identical to those obtained experimentally

Mass spectrometry (MS)

Mass analyses of the peptides were performed in positive ionization mode using a Micromass Q-TOF micro mass spectrometer (Waters) equipped with an electrospray ion source in the 150–2,000 Da range. A mixture of acetonitrile and water (1:1) containing 0.1 % formic acid was continuously delivered to the ion source at a 0.1-mL/min flow rate. Samples dissolved in the mobile phase were introduced using a 2-μL loop. The capillary voltage, cone voltage, desolvation temperature, and source temperature were 3.5 kV, 20 V, 150 and 90 °C, respectively.

Peptide sequencing by Edman degradation

The N-terminal amino acid sequence was determined on the Procise Protein Sequencing System (PE Applied Biosystems, 491 Protein Sequencer, Foster City, CA, USA) using the manufacturer's pulse-liquid Edman degradation chemistry cycles.

Determination of disulfide bridges pattern

Native PNG-R isolated from the venom extract as an HPLC peak (Fig. 1) was dissolved in 0.1 M MES buffer (pH 6.5) containing 2-mM $CaCl_2$ (50 μL). After addition of 1 μL of thermolysin stock solution in water (1 mg/mL), the mixture was incubated at 37 °C for 16 h. The reaction was quenched using 10 % TFA (2 μL) and then the mixture was fractionated by RP-HPLC using a linear gradient from 5 to 70 % acetonitrile/water/0.1 % TFA over 60 min. The peptide fragments detected at 220 nm (Fig. 2) were collected and then analyzed by MS. The patterns of disulfide bridges of synthetic PNG-K and PNG-R were determined similarly.

Peptide synthesis

Panurgines and their analogs were synthesized manually using a solid-phase method according to the N^{α}-Fmoc chemistry protocol in 5-mL polypropylene syringes with a Teflon filter at the bottom. Syntheses of PNG-1 and its analogs were carried out on Rink Amide MBHA resin (110 mg), while the linear forms of PNG-K, PNG-K/1, PNG-R, and PNG-R/1 were assembled on a 2-chlorotrityl chloride resin (110 mg). All four cysteine residues were incorporated into the sequences using Fmoc-Cys(Trt)-OH

derivative. Fmoc amino acids (4 eq, 0.28 mmol) were coupled using *N*,*N*'-diisopropylcarbodiimide (DIPC, 7 eq, 0.49 mmol) and 1-hydroxybenzotriazole (HOBt, 5 eq, 0.35 mmol) as coupling reagents in *N*,*N*'-dimethylformamide (DMF, 0.6 mL) as solvent. The free amino group conversion during the coupling was monitored with 1 % bromphenol blue indicator in DMF (1 μL). Deprotections of the α-amino group were performed with 20 % piperidine in DMF. PNG-1 and its analogs as well as PNG-K/1 and PNG-R/1 were fully deprotected and cleaved from the resin with a 2-mL mixture of TFA/H_2O/triisopropylsilane (95:2.5:2.5), while cysteine-containing linear precursors of PNG-R and PNG-K were cleaved with a 2-mL mixture of TFA/thioanisole/H_2O/1,2-ethanedithiol/triisopropylsilane (90:3:2.5:2.5:2) for 3.5 h and then the peptides were precipitated with *tert*-butyl methyl ether. Crude peptides of PNG-1 series and PNG-R/1 and PNG-K/1 were further purified by preparative HPLC using a Vydac C-18 column (10 × 250 mm; 5 μm) at a 3-mL/min flow rate using the solvent gradient as described above. The purity and identity of peptide products were checked by analytical HPLC and electrospray ionization mass spectrometry (ESI–MS), respectively (Table 1).

Disulfide bonds formation of PNG-R and PNG-K

The crude linear fully deprotected peptides (40 mg) were dissolved in 0.1 M ammonium acetate buffer, pH 7.8 (100 mL, prepared by bubbling gaseous NH_3 into 0.1 M acetic acid), and stirred under open air at room temperature. The time course of the cyclization reaction was monitored by RP-HPLC. Typically, after 8 h of the reaction, the solvent

Table 1 Primary structures, MS data and RP-HPLC retention times (t_R) of PNG-1 and its analogs

Peptide	Sequence	Monoisotopic molecular mass (Da)		t_R (min)
		Calculated	Found[a]	
PNG-1	LNWGAILKHIIK-NH_2	1,403.9	1,403.7	31.44
PNG-1/1	NLWAGILKHIIK-NH_2	1,403.9	1,403.9	30.81
PNG-1/2	**K**NWGAILKHIIK-NH_2	1,418.9	1,418.7	25.79
PNG-1/3	L**K**WGAILKHIIK-NH_2	1,417.9	1,417.7	28.34
PNG-1/4	LN**K**GAILKHIIK-NH_2	1,345.9	1,345.7	20.54
PNG-1/5	LNW**K**AILKHIIK-NH_2	1,474.9	1,474.8	30.25
PNG-1/6	LNWG**K**ILKHIIK-NH_2	1,460.9	1,460.7	28.53
PNG-1/7	LNWGA**K**LKHIIK-NH_2	1,418.9	1,418.7	22.94
PNG-1/8	LNWGAI**K**KHIIK-NH_2	1,418.9	1,418.7	21.67
PNG-1/9	LNWGAILK**K**IIK-NH_2	1,394.9	1,394.8	32.11
PNG-1/10	LNWGAILKH**K**IK-NH_2	1,418.9	1,418.7	23.64
PNG-1/11	LNWGAILKHI**K**K-NH_2	1,418.9	1,418.9	25.53
PNG-1/12	**K**NWG**K**ILKHIIK-NH_2	1,475.9	1,475.7	23.41
PNG-1/13	**K**NW**K**AILKHIIK-NH_2	1,490.0	1,490.0	24.64
PNG-1/14	LNWGA**V**LKH**VV**K-NH_2	1,361.8	1,361.6	26.37
PNG-1/15	LNWGA-**Abu**-LKH-**Abu**-**Abu**-K-NH_2	1,319.8	1,319.8	23.60
PNG-1/16	LNWGA**A**LKH**AA**K-NH_2	1,277.7	1,277.7	20.34
PNG-1/17	LNWGA**F**LKH**FF**K-NH_2	1,505.8	1,506.4	32.20
PNG-1/18	LNWGA**G**LKH**GG**K-NH_2	1,235.7	1,235.6	17.09
PNG-1/19	LNWGA**L**LKH**LL**K-NH_2	1,403.9	1,403.8	32.64
PNG-1/20	LNWGA-**Nle**-LKH-**Nle**-**Nle**-K-NH_2	1,403.9	1,403.9	33.01
PNG-1/21	LNWGA-**Aca**-LKH-**Aca**-**Aca**-K-NH_2	1,439.9	1,440.0	33.06
PNG-1/22	LNWGA**W**LKH**WW**K-NH_2	1,622.9	1,622.8	31.13
PNG-K	LDVKKIICVACKIKPNPACKKICPK	2,748.5	2,748.2	28.35
PNG-K/1	LDVKKII-**Abu**-VA-**Abu**-KIKPNPA-**Abu**-KKI-**Abu**-PK	2,680.8	2,680.3	24.38
PNG-R	LDVKKIICVACKIRPNPACKKICPK	2,776.5	2,776.5	28.74
PNG-R/1	LDVKKII-**Abu**-VA-**Abu**-KIRPNPA-**Abu**-KKI-**Abu**-PK	2,708.8	2,708.5	24.72

Bold letters show amino acid residues replaced; interchanged residues are shown underlined

Abu 2-aminobutyric acid, *Nle* norleucine, *Aca* 1-aminocyclohexane carboxylic acid

[a] See Supplementary Material for mass spectra

was removed by lyophilization and the desired cyclized product was purified by preparative RP-HPLC and characterized by MS (Table 1).

Determination of antimicrobial and hemolytic activity

A qualitative estimate of antimicrobial properties was undertaken using the drop diffusion test on Petri dishes by the double layer technique. Minimum inhibitory concentrations (MICs) were established by observing bacterial growth in multi-well plates (Čeřovský et al. 2008a, b, 2009; Monincová et al. 2010). Mid-exponential phase bacteria were added to individual wells containing solutions of the peptides at different concentrations in LB broth (0.5 % NaCl) in final volume of 0.2 mL and final peptide concentration in the range of 0.5–100 μM. The plates were incubated at 37 °C for 20 h, while being continuously shaken in a Bioscreen C instrument (Oy Growth Curves AB Ltd., Helsinki, Finland). The absorbance was measured at 540 nm every 15 min and each peptide was tested at least three times in duplicates. Routinely, 1×10^4 to 5×10^4 CFU of bacteria per well were used to determine the activity. Tetracycline in the 0.5–50 μM concentration range was tested as a standard. Antimicrobial testing in a reducing environment was done in the presence of 1.25-mM dithiothreitol (DTT).

Hemolytic activity was expressed as a concentration of a peptide able to lyze 50 % of human erythrocytes in the assay (LC_{50} values) as described by Monincová et al. (2010). Briefly, the peptides were incubated with red blood cells of healthy volunteers for 1 h at 37 °C in a physiological solution at a final volume of 0.2 mL (final erythrocyte concentration 5 % (v/v) and final peptide concentration 1–200 μM). The samples were then centrifuged for 5 min at 250 g and the supernatant absorbance determined at 540 nm. Supernatants of red blood cells suspended in physiological solution and in 0.2 % Triton X100 in physiological solution served as controls for zero and 100 % hemolysis, respectively. Each peptide was tested in duplicate in at least two independent experiments.

Circular dichroism

Circular dichroism (CD) spectra were collected by Jasco 815 spectrometer (Tokyo, Japan) in spectral range 190–300 nm using a 0.1 cm quartz cell at room temperature. The experimental setup was as follows: 5-nm step resolution, 20-nm/min scanning speed, 8-s response time, 1-nm spectral band width. The final peptide concentration was kept constant (0.25 mg/mL) for all peptides studied. All peptides were measured in water and in water/trifluoroethanol (TFE) mixtures (from 10 to 50 % v/v of TFE) and in the presence of SDS at concentrations of 0.016–8 mM (below and above the critical micelles concentration—cmc). After baseline correction, the final spectra were expressed as a molar ellipticity θ (deg cm^2 dmol^{-1}) per residue. The α-helix fraction (f_h) was calculated assuming a two-state model (Backlund et al. 1994; Rohl and Baldwin 1998) for linear PNG-1 peptides. In the case of disulfide-containing PNG-K(R), an online circular dichroism analysis program, Dichroweb (http://dichroweb.cryst.bbk.ac.uk), was used in data analysis (Whitmore and Wallace 2008).

Preparation of phospholipid vesicles (LUVs) with entrapped calcein

Vesicles were prepared from DOPC/DPPG (1:2, mol/mol), DOPC/DOPG (1:2, mol/mol), DOPC and DOPE/DOPG/CL (15:80:5, mol/mol/mol) lipids. Lipid films were made by dissolving appropriate amounts of lipids in chloroform (typically in 1 mL), except vesicles 1:2 DOPC/DPPG, for which a mixture of chloroform/methanol (3:1) was used. The solvent was then evaporated by a stream of nitrogen to deposit lipids as a film on the wall of the test tube. Dried thin lipid films were further vacuum dried overnight to completely remove the residual organic solvent. Large unilamellar vesicles (LUVs) with entrapped calcein were prepared by vortexing the dried lipids in 1 mL of dye buffer solution (70-mM calcein in 50-mM $Na_2HPO_4 \cdot 2H_2O$ containing 150-mM NaCl and 1-mM EDTA, pH 7.4). The suspension of that composition was further processed with five cycles of freezing and thawing, and subsequently extruded 31 times through a 100-nm pore size polycarbonate membrane (Nuclepore Track-Etched Membranes, Avanti Polar Lipids, Alabama) using a Mini-Extruder (Avanti Polar Lipids). The size distribution of resulting LUVs was characterized by dynamic light scattering (data not shown) with a Malvern Zetasizer Nano (Zen 3600, 633-nm red laser, Malvern Laboratories, Malvern, UK). The non-entrapped calcein was removed using a mini-column centrifugation method in a plastic syringe (3 × 5 cm, plugged with filter pad) filled with hydrated Sephadex G-50 coarse gel. Vesicle suspension (400 μL) was added dropwise on top of the gel in the syringe and the calcein-entrapped vesicles were eluted by centrifugation at 2,000 rpm for 10 min. The non-entrapped calcein remained bound to the gel, while vesicles passed through the gel and were collected.

Calcein leakage measurement

The leakage of calcein from the LUVs was monitored by measuring fluorescence intensity at an excitation wavelength of 490 nm and an emission wavelength of 520 nm on a Tecan Infinite 200 spectrometer (Tecan Group Ltd., Männedorf, Switzerland). Particular mixtures of AMPs and

LUVs for calcein leakage measurement contained 50 μL of the given peptide concentration and 50 μL of calcein-entrapped liposomes (32 μM). For determination of 100 % dye release, 10 % Triton X-100 in a buffer (50 μL) was used. The percentage of calcein leakage caused by AMPs was calculated using the equation $100 \times (F - F_0)/(F_t - F_0)$, where F is the fluorescence intensity gained by AMPs treatment, and F_0 and F_t are the intensities without AMPs and after Triton X-100 treatment, respectively (Chou et al. 2010). Each peptide was tested in at least five independent experiments.

Transmission electron microscopy

The effect of antibacterial peptide PNG-1/21 on the structure of *B. subtilis* cells was studied by negative staining method. Bacterial suspension after treatment with the peptide for 60 min, and untreated bacteria as a control, was adsorbed on carbon-stabilized Parlodion-coated copper grids for 5–10 min. After short washing, the samples were negatively stained by floating on a drop of 0.25 % aqueous phosphotungstic acid with 0.01 % bovine serum albumin for 30 s. Excess stain was blotted off with a piece of filter paper and samples were air dried. A JEOL JEM 1011 transmission electron microscope operating at 60 kV was used for analysis.

Results and discussion

Peptide isolation and primary structure determination

The RP-HPLC profile at 220 nm of the venom extract obtained from the eight venom reservoirs shows several peaks (Fig. 1). The components of the three most intense ones labeled as PNG-K, PNG-R and PNG-1 (PNGs) exhibited antimicrobial activity against *M. luteus*. The UV spectra corresponding to those peaks indicated the presence of peptides lacking aromatic amino acid residue in the sequences of PNG-R and PNG-K, and the presence of Trp residue within the sequence of PNG-1. The molecular masses of PNGs measured by internally calibrated ESI-QTOF MS were calculated manually from the *m*/*z* values of the monoisotopic peaks (the first one in the isotopic distribution of multiple charged cluster) of molecular ions found in their mass spectra (Fig. 1 of Supplementary Material). That resulted in monoisotopic molecular masses of 2,748.5 for PNG-K, 2,776.3 for PNG-R, and 1,403.7 for PNG-1. The Edman degradation (see Supplementary Material) gave entire sequences as follows: LDVKKIIXV AXKIKPNPAXKKIXPK (PNG-K), LDVKKIIXVAXKIR PNPAXKKIXPK (PNG-R), and LNWGAILKHIIK (PNG-1). In the cases of PNG-K and PNG-R, we assumed that all four undetermined amino acid residues (X) at positions 8, 11, 19, and 23 were cysteines forming disulfide bridges. The molecular masses of PNGs calculated on the bases of the sequences determined by Edman degradation corresponded to those values determined by MS. The determined deconvoluted masses signify that PNG-K and PNG-R are not C-terminally amidated, unlike the C-terminally amidated PNG-1.

The pattern of disulfide bridges in PNG-K and PNG-R was determined by the ESI–MS identification (Fig. 2 of Supplementary Material) of peptide fragments isolated by HPLC from their thermolysin digests. Among several fragments, we clearly identified two peptides containing cystine (Fig. 2): IIC connected by disulfide bond to ICPK (Mr 804.4) and cyclic fragment with intramolecular disulfide bond VACKIXPNPACKK (Mr 1,396.5 for X=K and Mr 1,424.8 for X=R). Sequences of these two fragments clearly fit to the sequences of PNG-K and PNG-R with the pattern of disulfide bridges Cys8–Cys23, Cys11–Cys19.

The sequence of PNG-1 shows no significant homology to other known AMPs categorized in the antimicrobial peptide database (http://aps.unmc.edu/AP/main.php) (Wang et al. 2009) with the exception of halictine-2 (GKWMSLLKHILK), a peptide isolated previously in our laboratory from the eusocial bee *Halictus sexcinctus* (Monincová et al. 2010). The sequence comparison of PNG-K(R) with other AMPs found in the antimicrobial peptide database and also in the Basic Local Alignment Search Tool (BLAST) program at (http://blast.ncbi.nlm.nih.gov/Blast.cgi) shows no homology to other known peptides. PNG-K(R) peptides have considerable content of hydrophobic residues (9) and high net positive charge (+7). This combination of amino acids is a prerequisite for antimicrobial properties. It is notable that the PNG-K(R) peptides display no homology with the neurotoxic peptide apamin (Labbé-Julié et al. 1991) from the venom of honeybees, which contains two disulfide bridges, nor to lasiocepsin, the AMP identified in the venom of the eusocial bee *L. laticeps* composed of 27 amino acid residues and two disulfide bridges (Monincová et al. 2012). The full biological role of PNGs in the venom of *P. calcaratus* is still unknown, except that they are antimicrobial.

Peptide synthesis and design of analogs

PNG-1 and its analogs were prepared by standard Fmoc chemistry on Rink amide MBHA resin, yielding an average 100 mg of crude peptide products. For further studies, this material was purified by preparative RP-HPLC to provide peptides of analytical HPLC purity ranging from 96 to 99 %. The retention times and the results of MS analyses confirming their identities are shown in Table 1. PNG-1,

belonging to the category of linear amphipathic α-helical peptides (Fig. 3), is cationic (net charge +3) due to the presence of two lysine residues and absence of acidic residues. Its cationicity in combination with seven hydrophobic amino acid residues presented in the sequence renders its antimicrobial properties.

To follow the effect of cationicity, amphipathicity, and hydrophobicity on the biological activity and disruption of the LUVs, we designed several analogs in which we (1) interchanged Leu1 with Asn2, and Gly4 with Ala5 in the sequence, thus, obtaining the ideal amphipathic helical peptide; (2) conducted a lysine scan to examine the effect of the incorporation of an additional positive charge into different positions; (3) replaced both Leu1 and Gly4 as well as Leu1 and Ala5 by Lys, thus resulting in two analogs, each having two additional positive net charges (Fig. 3 of Supplementary Material); and (4) replaced all Ile residues in the positions 6, 10, and 11 by a series of different amino acid residues to support our assumption as to the importance of the presence of Ile residues in amphipathic α-helical peptides for antimicrobial activity.

Linear precursors of PNG-K and PNG-R and their corresponding analogs PNG-K/1 and PNG-R/1 which have all Cys residues substituted by 2-aminobutyric acid (Abu) were prepared on 2-chlorotrityl chloride resin by the same procedure as described above. PNG-K/1 and PNG-R/1 were further purified by preparative RP-HPLC, while the Cys-containing fully deprotected PNG-K and PNG-R were subjected in their crude form to an air-mediated cyclization reaction (formation of disulfide bridges) as described in experimental section. The oxidative folding of crude linear precursor of PNG-K, showing one dominant HPLC peak (Fig. 4a of Supplementary Material), resulted during 12 h of oxidation in the formation of a major cyclic product eluted at a longer retention time than its linear precursor and that corresponded to the parent native PNG-K peptide (Fig. 4b of Supplementary Material). ESI–MS analysis of this product revealed a loss of four mass units compared to its linear precursor (Fig. 5 of Supplementary Material). However, HPLC analysis of the crude linear PNG-R precursor showed, in addition to the expected linear peptide (Mr = 2,780.6), a mixture of several peptides which were identified by ESI–MS as spontaneously oxidatively folded isomers (Mr = 2,776.3). When that entire mixture was subjected to oxidative folding by an air-mediated cyclization reaction, those isomers converted into one major cyclic required peptide product during 12 h of oxidation. It had the same retention time as that of parent native PNG-R, and its determined molecular mass (Mr = 2,776.3) corresponded to its calculated value. Mass spectra of HPLC purified PNG-K and PNG-R are shown in Supplementary Material as Figs. 5 and 6. The pattern of their disulfide bridges (identical to that of natural peptides) which is Cys8–Cys23, Cys11–Cys19 was verified by identification of peptide fragments isolated from thermolysin digest (Figs. 7 and 8 of Supplementary Material). The above results show that the disulfide bonds formation in PNG-K(R) could be easily accomplished in one-pot cyclization/folding reaction, while avoiding the methods utilizing selective cysteines protection. We have also succeeded with that strategy in the case of insect defensin presenting three disulfide bridges (Čeřovský et al. 2011).

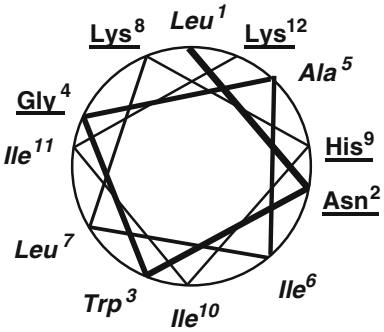

Fig. 3 Wheel diagram of PNG-1. Hydrophobic amino acid residues in *bold italic*, hydrophilic residues *underlined*

Biological activity

PNG-1 shows high antimicrobial activity against the sensitive Gram-positive bacteria *M. luteus* and *B. subtilis* and slightly lower activity against pathogenic *S. aureus* (Table 2). The activity against Gram-negative *E. coli* was also high, but pathogenic *P. aeruginosa* was somewhat more resistant. Toxicity to human red blood cells determined as LC_{50} value in a hemolytic test was moderate. PNG-1 displays potent killing activity against *C. albicans* (Table 2).

Although PNG-1 exhibits antimicrobial activities comparable to those of other known AMPs of that category and size, its moderate hemolytic activity is not satisfactory with respect to therapeutic potential. In agreement with the literature, antimicrobial activity of α-helical peptides depends on their net cationic charge (Jiang et al. 2008), which is required for the electrostatic attraction of a peptide to the negatively charged phospholipids of bacterial cell membrane, and on moderate hydrophobicity and flexibility. Hemolytic activity is related more to the hydrophobicity (Chen et al. 2007) and helical structure (Wieprecht et al. 1997). The formation of the helical structure of the peptide is, however, an important means for the adoption of its amphipathic structure.

Exchanging the order of Leu1 with Asn2 and Gly4 with Ala5 in the sequence of PNG-1 resulting in the PNG-1/1 analog of ideal amphipathic helical structure (Fig. 3 of

Table 2 Antimicrobial and hemolytic activity of PNGs and their analogs

Peptide	Antimicrobial activity MIC (μM)						Hemolytic activity LC_{50} (μM)
	M.l.	*B.s.*	*S.a.*	*E.c.*	*P.a.*	*C.a*	
PNG-1	1.5	1.3	10.6	3.7	51.7	7.3	119
PNG-1/1	2.5	4.5	36.7	12.5	>100	10.8	>200
PNG-1/2	9	5.8	100	17.1	83.3	9.8	>200
PNG-1/3	3.7	3.7	11.7	3.7	46.7	5.1	>200
PNG-1/4	100	65	>100	>100	>100	100	>200
PNG-1/5	1.3	1.3	5.3	2.3	14.3	4.0	~110
PNG-1/6	2.2	1.7	8.7	4.0	20.8	7.3	>140
PNG-1/7	38.8	55.8	>100	>100	>100	50	>200
PNG-1/8	46.7	58.3	>100	>100	>100	75	>200
PNG-1/9	2.7	2.0	7.3	4.3	43.3	6	>200
PNG-1/10	30	41.7	>100	>100	>100	>100	>200
PNG-1/11	10.8	13.3	100	70	93.3	11.3	>200
PNG-1/12	4.5	5.8	76.7	11.3	31.7	7.7	>200
PNG-1/13	5	2.5	65	7.8	65	8	>200
PNG-1/14	8.2	23.0	>100	90.0	>100	31.7	>200
PNG-1/15	35.0	47.0	>100	>100	>100	>100	>200
PNG-1/16	100	>100	>100	>100	>100	>100	>200
PNG-1/17	3.5	3.3	21.7	5.0	76.7	7.2	81.0
PNG-1/18	100	>100	>100	>100	>100	>100	>200
PNG-1/19	2.2	1.6	6.7	3.8	40.0	6.7	63.0
PNG-1/20	2.5	2.0	5.0	4.0	57.0	5.0	40.0
PNG-1/21	1.8	1.8	5.8	3.0	43.0	6.0	43.0
PNG-1/22	2.5	2.3	20.0	7.2	100	14.2	132
PNG-K	1.6	3.3	>100	63.3	>100	24.2	>200
PNG-K/1	50	>100	>100	>100	>100	>100	>200
PNG-R	0.8	1.5	>100	32.5	>100	18.7	>200
PNG-R/1	19.2	>100	>100	>100	>100	>100	>200

M.l. Micrococcus luteus, *B.s. Bacillus subtilis*, *S.a. Staphylococcus aureus*, *E.c. Escherichia coli*, *P.a. Pseudomonas aeruginosa*, *C.a. Candida albicans*

Supplementary Material) reduced its antimicrobial activity, but improved its hemolytic properties.

To follow the effect of increasing cationicity on biological activity, we prepared a series of PNG-1 analogs in which one or two amino acid residues were substituted by Lys. The successive replacement of each of the ten non-Lys residues by Lys in the PNG-1 (lysine scan) resulted in diverse biological activities. Generally, such change made within the hydrophobic segment (Fig. 3 of Supplementary Material) of the α-helix (Trp3, Ile6, Leu7, Ile10, Ile11) decreased drastically the antimicrobial potency of the peptide as well as its hemolytic activity. This is due to significant decrease in peptide amphipathicity. The substitution of hydrophobic residues located in the hydrophilic segment (Leu1, Ala5) with Lys making both analogs (PNG-1/2, PNG-1/6) more cationic and more amphipathic did not have such a prominent effect on the biological activities. The PNG-1/2 analog exhibited decreased antimicrobial potency against pathogenic *S. aureus* and improved hemolytic properties, while the PNG-1/6 analog exhibited increased potency against *P. aeruginosa* and a slight decrease of hemolytic activity. On the other hand, the replacement of hydrophilic residues (Asn2, Gly4 and His9) by Lys in the hydrophilic segment, thus maintaining the amphipathicity of the peptide, resulted in the analogs showing a trend of increasing antimicrobial potency and decreasing hemolytic activity. The increase of hemolytic activity in parallel with the gain in antimicrobial activity against pathogenic *S. aureus* and *P. aeruginosa* reflected the substitution of Gly4 (a slight helix breaker) by the α-helix-promoting Lys residue. The analog obtained by the substitution of His9 (PNG-1/9) within the hydrophilic segment exhibited lower hemolytic activity while preserving its antimicrobial properties.

Simultaneous replacement of two amino acid residues by Lys within the hydrophilic segment produced cationic

peptides of net charge +5 (PNG-1/12, PNG-1/13) that show a decrease in antimicrobial potency against *S. aureus* but negligible hemolysis.

To evaluate the effect of hydrophobicity and amphipathicity on biological activity and to support our assumption as to the importance for biological activity of Ile residues presented in short amphipathic α-helical AMPs, we designed several analogs of PNG-1 in which we replaced all Ile residues in the positions 6, 10 and 11 with different non-polar amino acid residues. Replacement of all Ile residues by isosteric Leu or Nle produced the PNG-1/19 and PNG-1/20 analogs, respectively, with antimicrobial activity slightly increased against *S. aureus*, while the activities against other microbes were unchanged. Their hemolytic activities, however, increased two- to threefold. Replacing the Ile residues with more bulky and hydrophobic Phe (PNG-1/17) and Trp (PNG-1/22) residues resulted in an apparent decrease of antimicrobial activity against all microbes tested and preservation of the hemolytic activity. Decreasing peptide hydrophobicity by replacing Ile residues with Abu, Val, Ala and Gly resulted either in a significant decrease of potency against all microorganisms tested (PNG-1/14, PNG-1/15) or in a total loss of any activity (PNG-1/16, PNG-1/18). In parallel, those four analogs also lost hemolytic activity. Placing hydrophobic and sterically hindered 1-aminocyclohexane carboxylic acid into those positions rendered the PNG-1/21 analog with slightly improved antimicrobial activities, but increased hemolytic activity. Based on our observations, we assume that the existence of Ile residues in shorter linear α-helical amphipathic AMPs at certain positions represents the best selection given to these peptides by nature. Decrease of hydrophobicity followed in the series of PNG-1 analogs correlates with decrease of their hemolytic activities and with their retention times as measured by RP-HPLC. All peptides eluted with retention time <30 min showed weak hemolytic activity ($LC_{50} > 200$).

The disulfide bridges containing PNG-K and PNG-R peptides exhibited strong antimicrobial activity against sensitive Gram-positive *M. luteus* and *B. subtilis* but weak activity against *E. coli*, while both peptides were

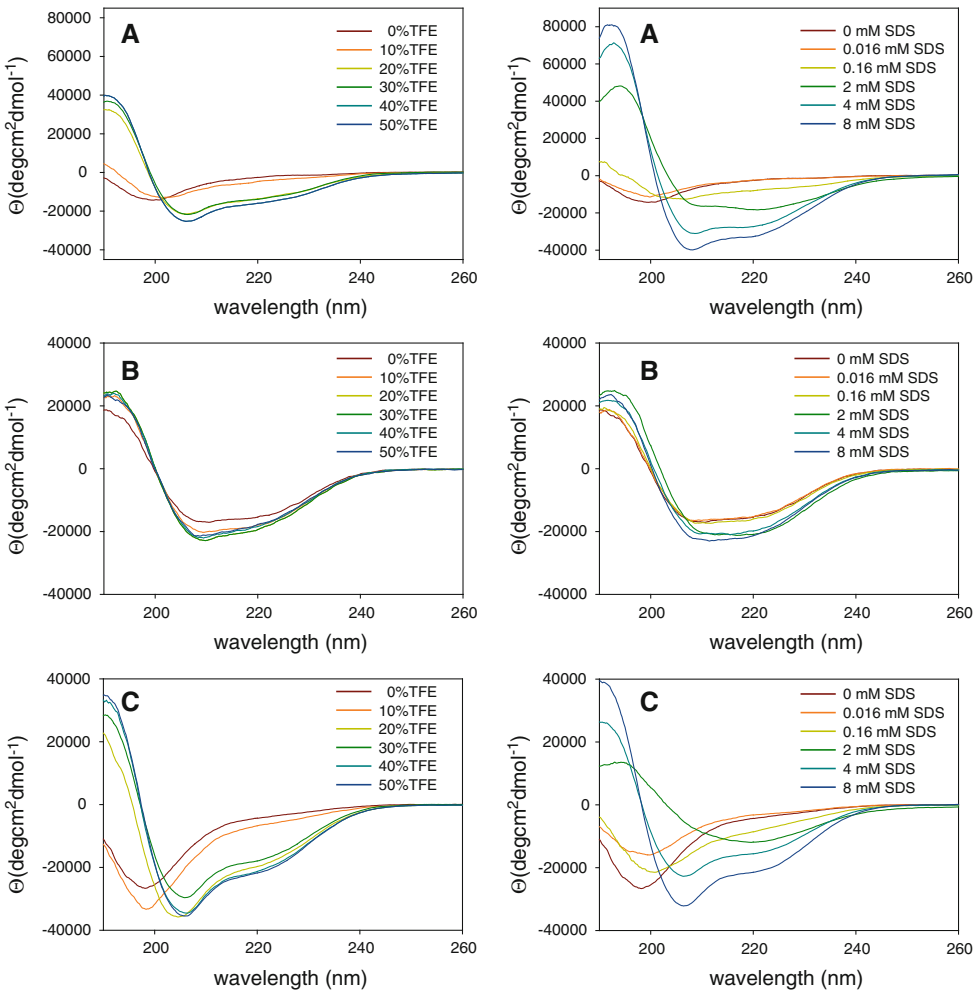

Fig. 4 UV CD spectra of PNG-1 (**a**), PNG-R (**b**) and PNG-R/1 (**c**) in the presence of various concentrations of TFE (*left panels*) and SDS (*right panels*). CD spectra of PNG-K and PNG-K/1 exhibit very similar profiles as **b** and **c**, respectively (not shown)

Table 3 Calculated α-helical fractions (f_h, in percentages) of PNG-1 and selected analogs determined by CD spectroscopy in the presence of varying concentrations of TFE

Peptide	Sequence	α-Helical fraction (f_h)					
		TFE (%)					
		0	10	20	30	40	50
PNG-1	LNWGAILKHIIK-NH_2	14	19	40	40	46	46
PNG-1/1	NLWAGILKHIIK-NH_2	13	17	36	46	64	70
PNG-1/6	LNWGKILKHIIK-NH_2	13	17	31	39	40	37
PNG-1/12	KNWGKILKHIIK-NH_2	11	13	26	30	31	31
PNG-1/14	LNWGAVLKHVVK-NH_2	13	16	41	46	52	56
PNG-1/15	LNWGA-Abu-LKH-Abu-Abu-K-NH_2	9	14	25	32	34	34
PNG-1/16	LNWGAALKHAAK-NH_2	8	11	19	26	28	29
PNG-1/17	LNWGAFLKHFFK-NH_2	8	15	25	29	28	28
PNG-1/18	LNWGAGLKHGGK-NH_2	8	8	9	10	11	12
PNG-1/19	LNWGALLKHLLK-NH_2	14	28	41	42	42	42
PNG-1/20	LNWGA-Nle-LKH-Nle-Nle-K-NH_2	13	24	39	40	41	41
PNG-1/21	LNWGA-Aca-LKH-Aca-Aca-K-NH_2	16	24	32	33	34	34
PNG-1/22	LNWGAWLKHWWK-NH_2	17	18	18	16	15	15

Table 4 Calculated α-helical fractions (f_h, in percentages) of PNG-1 and selected analogs determined by CD spectroscopy in the presence of varying concentrations of SDS

Peptide	Sequence	α-Helical fraction (f_h)					
		SDS (mM)					
		0	0.016	0.16	2	4	8
PNG-1	LNWGAILKHIIK-NH_2	14	14	27	53	72	84
PNG-1/1	NLWAGILKHIIK-NH_2	13	13	22	49	72	95
PNG-1/6	LNWGKILKHIIK-NH_2	15	16	18	61	59	54
PNG-1/12	KNWGKILKHIIK-NH_2	11	12	16	58	55	47
PNG-1/14	LNWGAVLKHVVK-NH_2	13	13	16	46	57	67
PNG-1/15	LNWGA-Abu-LKH-Abu-Abu-K-NH_2	11	11	13	50	46	36
PNG-1/16	LNWGAALKHAAK-NH_2	10	9	9	39	33	30
PNG-1/17	LNWGAFLKHFFK-NH_2	9	11	14	29	31	30
PNG-1/18	LNWGAGLKHGGK-NH_2	8	8	8	12	11	11
PNG-1/19	LNWGALLKHLLK-NH_2	15	15	19	50	48	39
PNG-1/20	LNWGA-Nle-LKH-Nle-Nle-K-NH_2	15	15	21	52	53	47
PNG-1/21	LNWGA-Aca-LKH-Aca-Aca-K-NH_2	17	17	20	45	40	39
PNG-1/22	LNWGAWLKHWWK-NH_2	20	19	17	36	33	32

inactive against pathogenic *S. aureus* and *P. aeruginosa* and were not hemolytic. The linear analogs (PNG-K/1 and PNG-R/1) having all four Cys residues replaced by Abu were inactive against all bacteria tested with the exception of noticeable activity against the most sensitive *M. luteus*. On the other hand, the linear PNG-K peptide with all –SH groups in reduced form showed antimicrobial activity similar to that of parent PNG-K when tested against *M. luteus* and *B. subtilis*. We may speculate that linear PNG-K was oxidatively folded when performing the assay. When carrying out the parallel assay in the presence of reducing agent 1,4-dithiothreitol (DTT) to prevent the effect of spontaneous oxidative folding, the activity of linear reduced peptide was surprisingly similar to that of the presumably oxidized peptide (experiment without DTT). That behavior of linear PNG-K/1 is analogous to the behavior of the linear version of lasiocepsin, a disulfide bridges containing AMP identified in our laboratory from the venom of another wild bee (Monincová et al. 2012).

Table 5 Percentages of secondary structures in PNG-K, PNG-R and in their corresponding linear analogs PNG-K/1 and PNG-R/1 determined by CD spectroscopy relative to varying concentrations of TFE and SDS

Peptide	Secondary structures (%)											
	TFE (%)						SDS (mM)					
	0	10	20	30	40	50	0	0.016	0.16	2	4	8
PNG-K												
Helix	54	63	62	64	66	66	54	63	66	72	76	75
Sheet	10	7	7	6	6	7	10	7	6	6	4	5
Turn	17	16	16	16	16	15	17	16	15	13	14	13
Rnd. coil	20	17	16	15	14	17	20	16	15	21	12	14
PNG-K/1												
Helix	10	12	42	47	51	50	10	10	12	28	40	49
Sheet	57	53	19	16	13	15	57	57	53	19	16	13
Turn	17	18	20	20	20	20	17	18	17	16	18	19
Rnd. coil	16	18	19	17	15	17	16	16	18	38	26	20
PNG-R												
Helix	46	55	46	60	57	56	46	55	47	59	56	56
Sheet	13	8	13	8	8	9	13	9	12	7	8	8
Turn	18	16	18	17	17	17	18	17	17	15	16	16
Rnd. coil	23	19	23	16	17	18	23	17	24	22	20	20
PNG-R/1												
Helix	10	10	59	62	74	77	10	11	11	30	56	56
Sheet	57	58	13	9	6	5	57	51	51	18	10	10
Turn	17	18	21	19	17	17	17	17	17	16	18	18
Rnd. coil	17	14	7	10	6	6	17	21	21	36	16	16

CD spectra and conformation

In water, PNG-1 exhibited CD spectra that are characteristic of an unstructured peptide with a broad minimum at 200 nm of low intensity (Fig. 4a), containing approximately 14 % α-helix (Table 3). The CD spectra underwent a considerable change with increasing concentration of TFE or SDS, demonstrating a predominantly α-helical structure as indicated by the appearance of typical bands at 208 and 222 nm (Fig. 4a). The spectra show a maximum α-helical content of 46 % in solution containing 40 % of TFE, and 84 % at 8 mM of SDS (Tables 3, 4). CD spectra of some structurally related PNG-1 analogs (PNG-1/6, PNG-1/14, PNG-1/15, PNG-1/16, PNG-1/17, PNG-1/19, PNG-1/20, and PNG-1/21) display profiles similar to those of the parent peptide, but indicating less pronounced propensity to form α-helix with increasing concentration of TFE or SDS (Fig. 9 Supplementary Material for their CD spectra). These analogs adopted also a maximal α-helical conformation at 40 % TFE (which remained unchanged at higher concentration of TFE) or in the presence of SDS around cmc (2–4 mM), which decreased above this concentration (Tables 3, 4). Spectral changes observed above cmc could be explained in terms of additional formation of polyproline II structure (Pazderková et al. 2012). Surprisingly, replacement of all Ile residues in PNG-1 by isosteric Leu residues (PNG-1/19) showed a similar ability to form helical structure in SDS concentration around cmc, but the helical content above cmc was only about one-half that (40 %) of the parent peptide (84 %). On the other hand, the spectra of PNG-1/18 clearly reflect the presence of three Gly residues as helix breaker in the peptide sequence and preventing helix formation even at high concentrations of TFE or SDS. The spectra of PNG-1/17 in the presence of 0.16 mM SDS (Fig. 9 of Supplementary Material) indicate the formation of a β-sheet structure among the unordered molecules, and at higher concentration of SDS, the shape of the spectral curves indicates a mixture of secondary structures including both helical and β-sheet structures. The PNG-1/21 analog, having replaced Ile residues by α,α-dialkylated, conformationally restricted 1-aminocyclohexane carboxylic acid (Aca), did not exhibit the expected propensity to form a helical structure in the presence of helix promoters. The tryptophan-rich PNG-1/22 analog showed unordered structure in water with α-helical content 20 % and which increased in the presence of SDS around cmc (2–4 mM). Nevertheless, its spectral curves obtained at the higher concentration of TFE indicate no effect of increasing its helical content. The PNG-1/1 analog of ideal amphipathic helical structure exhibited the highest helical content of all analogs studied at high concentration of TFE and SDS (Tables 3, 4).

The peptides with no Ile residues substituted (PNG-1, PNG-1/1) exhibited highest helicity of all studied peptides in the anisotropic environment of SDS micelles and at high TFE concentration. This would be in contradiction with the published data showing the order of helix-forming propensity of aliphatic amino acid residues being Nle ≡ Ala > Abu > Leu > Ile > Val, from which Ile and Val are considered as weakly destabilizing residues (Lyu et al. 1991). That measurement, however, had been carried out in 10-mM salt solution.

The CD spectra of PNG-K and PNG-R peptides containing two disulfide bridges show that they become structured already in water with helical content around 54 and 46 %, respectively (Table 6; Fig. 4b), which did not increase significantly with the increments of TFE concentration. The increase of α-helical content was more prominent in the presence of SDS at cmc and above. According to data analysis (Whitmore and Wallace 2008), the increase of helical content was at the expense of decreased β-sheet and β-turns of the peptide, but a correct and detailed interpretation of this set of CD spectra (Fig. 4b) is a rather complicated matter.

The linear peptides PNG-K/1 and PNG-R/1, having no disulfide bonds, exhibited substantially lower content of

Table 6 Minimal concentration of AMPs that cause 50 % calcein leakage from various liposomes

Peptide	Dye-leakage activity LC_{50} (μM)			
	DOPC/DOPG 1:2	DOPC/DPPG 1:2	DOPE/DOPG/CL 15:80:5	DOPC
PNG-1	2.4	1.0	3.5	4.8
PNG-1/1	2.0	1.3	1.8	6.2
PNG-1/6	1.2	0.8	1.4	4.1
PNG-1/12	2.0	1.4	1.1	7.0
PNG-1/14	2.2	1.4	1.4	31
PNG-1/15	>100	100.0	>100	>100
PNG-1/16	74	26	39	>100
PNG-1/17	2.4	0.8	2.4	6.9
PNG-1/18	>100	>100	>100	>100
PNG-1/19	1.3	0.5	1.4	2.0
PNG-1/20	1.3	0.9	1.8	2.7
PNG-1/21	1.2	0.6	1.3	1.3
PNG-1/22	3.6	0.9	3.6	2.2
PNG-K	0.7	0.8	0.7	>100
PNG-K/1	70	34	25	>100
PNG-R	0.7	0.8	0.7	100
PNG-R/1	70	26.5	23	>100

The data are averages of values obtained in five independent experiments

α-helix in water compared to their parent peptides. With the increasing concentration of TFE or SDS, however, their helical content increased considerably, thus indicating continuous formation of α-helix at the expense of β-sheet (Table 5; Fig. 4c). That is clearly indicated by the difference of spectral curves shape between PNG-K and PNG-R (Fig. 4b) versus their linear analogs PNG-K/1 and PNG-R/1 (Table 5; Fig. 4c), which show typical curves of α-helix. These results reflect the predicted secondary structures of PNG-K(R) obtained using the Protein Structure Prediction Server (PSIPRED) (Jones 1999), which indicates a content of the β-sheet in the N-terminal part of PNG-K(R) (residues 5–13), while the residues 17–21 represent α-helix (Fig. 10 of Supplementary Material). On the other hand, the prediction of secondary structure (based on the hypothetical substitution of Cys residues by Ala) of the PNG-K/1(R) shows the presence of two α-helical parts (residues 2–13 and 17–22). While α-helical structure is the essential structural component of PNG-K(R), with regard to their antimicrobial activity the presence of α-helix in the structure of PNG-K(R) is not the only requirement for the mechanism of these peptides' action. Their linear versions showed the ability to change secondary structure upon the addition of TFE or SDS, thus resulting in a remarkable increase of α-helical content even as they were inactive in the antimicrobial assay (Table 5).

Interaction of PNGs with LUVs

The membrane-permeabilizing activity of most studied peptides was tested by measuring the leakage of fluorescent dye calcein entrapped in LUVs. Calcein is self-quenching at high concentrations, and its fluorescence is increasing upon release from vesicles into medium and its dilution. We prepared negatively charged LUVs consisting of DOPC/DPPG (1:2) and DOPC/DOPG (1:2) as model lipid bilayers mimicking the bacterial cell membrane in general, as well as LUVs made from DOPE, DOPG, and CL in the ratio 15:80:5 mimicking the cell membrane of *B. subtilis*. The vesicles made solely from zwitterionic DOPC mimic the membrane of erythrocytes. Cationic AMPs usually exhibit membrane-permeabilizing activity preferentially against negatively charged liposomes, whereas their activity against neutral liposomes made from zwitterionic phospholipids is expected to be restricted (Chou et al. 2010). The dye-leakage activity of the AMPs expressed as an LC_{50} value (Table 6) was defined as the minimal concentration of AMPs required to cause 50 % of the calcein leakage from the LUVs (Chou et al. 2010).

PNG-1 and the majority of its analogs studied showed high dye-leakage activity against all LUVs tested, including those consisting of solely zwitterionic DOPC (Table 6). These activities roughly reflected the hydrophobicities and α-helicities of those peptides. Three analogs of this series—PNG-1/15, PNG-1/16, and PNG-1/18—having replaced all three Ile residues in the sequence of natural PNG-1 by less hydrophobic residues Abu, Ala and Gly, respectively, exhibited significantly low or no dye-leakage activity. These results correlate with the values for their biological activity as well as with their lower propensity to form α-helix in the presence of SDS micelles (especially PNG-1/18) with respect to parent PNG-1. Increasing the net positive charge of the peptide by +1 (PNG-1/6) or by +2 (PNG-1/12) as well as making the peptide of ideal amphipathic helical structure (PNG-1/1) had no additional effect on the dye-leakage activity. Surprisingly, the dye-leakage activity of PNG-1 and most of its analogs against neutral DOPC micelles was also high, but it still was markedly lower than were activities against negatively charged micelles. This may be attributed to hydrophobic interactions of peptides with lipidic bilayer of the vesicle membrane.

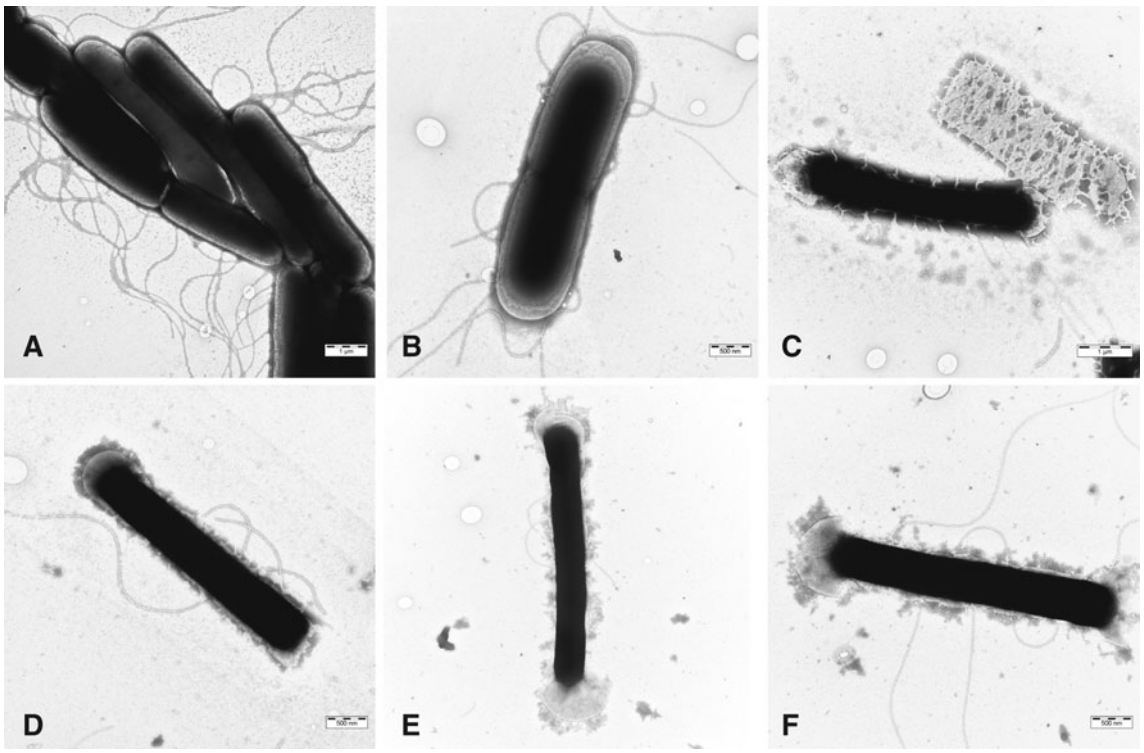

Fig. 5 Electron micrographs of negatively stained *Bacillus subtilis* either untreated (**a**, **b**) or treated by PNG-1/21 for 60 min (**c**–**f**) showing bacterial cells in different stages of disruption. *Scale bars* 1 μm (**a**, **c**), 500 nm (**b**, **d**–**f**)

On the other hand, both cationic cyclic PNG-K and PNG-R peptides showed profound differences between dye-leakage activity against negatively charged LUVs mimicking bacterial cell membranes and the neutral LUVs mimicking the membrane of a eukaryotic cell. Although inactive against most bacteria tested, their linear analogs (PNG-K/1 and PNG-R/1) still caused noticeable calcein leakage from negatively charged liposomes, but no leakage from neutral liposomes (Table 6).

All studied peptides showed slight preference to disrupt negatively charged micelles composed of phospholipids with dipalmitoyl acyl chains (DOPC/DPPG) rather than those composed of phospholipids with dioleyl acyl chain (DOPC/DOPG) (Table 6). That might be due to the different effect of those phospholipids to form liposomes with different "fluidity" of a lipid bilayer.

The dye-leakage activities of tested AMPs followed a trend similar to those of their antimicrobial and hemolytic activities. This is particularly noticeable in the case of those LUVs composed of DOPE/DOPG/CL corresponding to the *B. subtilis* membrane.

Transmission electron microscopy (TEM)

To examine the influence of PNG-1/21 on the morphology of Gram-positive bacteria (*B. subtilis* as a model system), we treated the bacterial cells with the peptide for 60 min. All samples were visualized by negative staining method. Bacteria in the untreated control revealed native morphology represented by electron-dense character and well-preserved bacterial membranes connected with many intact flagella (Fig. 5a, b). After treatment with PNG-1/21 for 60 min (Fig. 5c–f), many bacteria lost their flagella even though the inner part still revealed the electron-dense character in many of them. Only about 20 % of bacterial cells were electron-transparent with apparently disrupted structure (Fig. 5c). Those with still apparently electron-dense character showed altered cell membrane morphology in the middle part of the cells, which were shrunk (Fig. 5e, f). On the other hand, the envelope of both poles of the bacterial cells seemed to be swollen with some holes (Fig. 5d–f). The leakage of internal bacterial content from these polar ends was observed in many of peptide treated bacteria (Fig. 5c–f).

These phenomena might be explained by presence of higher amount of anionic phospholipids—cardiolipin (CL), localized at the septal and on the polar membranes of *B. subtilis* cells (Kawai et al. 2004). Cationic antibacterial peptide PNG-1/21 probably might react with anionic CL and promote their clustering, similarly as compounds that were found to be toxic to bacteria (Epand and Epand 2009). After peptide treatment, certain membrane domains localized on the both poles of bacterial cells, could be unstable and then damaged. Together with higher osmotic pressure

inside *B. subtilis* cells, this can result in swelling of the membranes on both bacterial poles leading finally to the leakage of internal bacterial contents. It is also obvious that the PNG-1/21 possesses strong affinity to the embedding of flagellas into the cell (Terashima et al. 2008) where the peptide probably disrupts cellular membrane in the tight vicinity of the flagellas.

Interestingly, we observed different action on the bacterial membrane of *B. subtilis* when we used other antibacterial peptides, lucifensin (Čeřovský et al. 2011) and lasiocepsin (Monincová et al. 2012). In the former case, we observed a leakage of the cytoplasmic content through many pores distributed over the entire bacterial surface. The latter case showed huge leakage of bacterial content from the holes prevalently localized at the ends of the bacterial cells.

Conclusion

In the course of our investigating AMPs isolated from the venom of Hymenoptera insects, we have found that the venom of wild bees offers a promising source of α-helical amphipathic peptides, such as, for example, PNG-1, which show potent antimicrobial properties and low or moderate toxicity to eukaryotic cells. In addition, some of those species contain in their venom cyclic AMPs containing disulfide bridges. Interestingly, none of those peptides displays any homology to apamin or melittin, the well-known peptides identified in the venom of honeybees. PNG-1, an α-helical peptide composed of 12 amino acid residues, is among the shortest linear cationic α-helical AMPs found in nature. This is an advantage in terms of its potential for chemical modification and possible applications. Increasing cationicity and amphipathicity of PNG-1 through substituting selected amino residues in the hydrophilic segment of the helix by lysine enhances the antimicrobial activity, particularly against *P. aeruginosa*, concomitant with a decrease in hemolytic activity. Any simultaneous substitution of the three Ile residues in the PNG-1 sequence resulted in the deterioration of its biological properties, thus indicating the importance of Ile residues presented in AMPs of this category. Cyclic PNG-K and PNG-R exhibit antimicrobial activity only against sensitive Gram-positive bacteria. Their potency to disrupt artificially made membrane mimicking cell membrane of bacteria was comparable to that of PNG-1, which was high. Unlike PNG-1, PNG-K(R) does not disrupt artificially made membranes that mimic membranes of eukaryotic cells.

Acknowledgments This work was supported by the Grant Agency of the Charles University no. 645012, Czech Science Foundation, Grant no. 203/08/0536, and by research project RVO 61388963 of the Institute of Organic Chemistry and Biochemistry, Academy of Sciences of the Czech Republic. We thank our technical assistants Mrs. Hana Hulačová and Mrs. Lenka Borovičková for their help with peptide synthesis. We also thank Gale A. Kirking at English Editorial Services, s.r.o. for assistance with the English.

Conflict of interest The authors declare that they have no conflict of interest.

References

Amiche M, Galanth C (2011) Dermaseptins as models for the elucidation of membrane-acting helical amphipathic antimicrobial peptides. Curr Pharm Biotechnol 12:1184–1193

Argiolas A, Pisano JJ (1985) Bombolitins, a new class of mast cell degranulating peptides from the venom of the bumblebee *Megabombus pennsylvanicus*. J Biol Chem 260:1437–1444

Asthana N, Yadav SP, Ghosh JK (2004) Dissection of antimicrobial and toxic activity of melittin. J Biol Chem 279:55042–55050

Backlund B-M, Wikander G, Peeters T, Graslund A (1994) Induction of secondary structure in the peptide hormone motilin by interaction with phospholipid vesicles. Biochim Biophys Acta 1190:337–344

Baltzer SA, Brown MH (2011) Antimicrobial peptides—promising alternatives to conventional antibiotics. J Mol Microbiol Biotechnol 20:228–235

Brandenburg L-O, Merres J, Albrecht L-L, Varoga D, Pufe T (2012) Antimicrobial peptides: multifunctional drugs for different applications. Polymers 4:539–560

Čeřovský V, Slaninová J, Fučík V, Hulačová H, Borovičková L, Ježek R, Bednárová L (2008a) New potent antimicrobial peptides from the venom of Polistinae wasps and their analogs. Peptides 29:992–1003

Čeřovský V, Hovorka O, Cvačka J, Voburka Z, Bednárová L, Borovičková L, Slaninová J, Fučík V (2008b) Melectin: a novel antimicrobial peptide from the venom of the cleptoparasitic bee *Melecta albifrons*. ChemBioChem 9:2815–2821

Čeřovský V, Buděšínský M, Hovorka O, Cvačka J, Voburka Z, Slaninová J, Borovičková L, Fučík V, Bednárová L, Votruba I, Straka J (2009) Lasioglossins: three novel antimicrobial peptides from the venom of the eusocial bee *Lasioglossum laticeps* (Hymenoptera: Halictidae). ChemBioChem 10:2089–2099

Čeřovský V, Slaninová J, Fučík V, Monincová L, Bednárová L, Maloň P, Štokrová J (2011) Lucifensin, a novel insect defensin of medicinal maggots: synthesis and structural study. ChemBioChem 12:1352–1361

Chen Y, Guarnieri MT, Vasil AI, Vasil ML, Mant CT, Hodges RS (2007) Role of peptide hydrophobicity in the mechanism of action of α-helical antimicrobial peptides. Antimicrob Agents Chemother 51:1398–1406

Chou H-T, Wen H-W, Kuo T-Y, Lin C-C, Chen W-J (2010) Interaction of cationic antimicrobial peptides with phospholipid vesicles and their antibacterial activity. Peptides 31:1811–1820

Epand RM, Epand RF (2009) Domains in bacterial membranes and the action of antimicrobial agents. Mol BioSyst 5:580–587

Epand RM, Epand RF (2011) Bacterial membrane lipids in the action of antimicrobial targets. J Pept Sci 17:298–305

Epand RF, Savage PB, Epand RM (2007) Bacterial lipid composition and the antimicrobial efficacy of cationic steroid compounds (Ceragenins). Biochim Biophys Acta 1768:2500–2509

Giuliani A, Pirri G, Nicoletto SF (2007) Antimicrobial peptides: an overview of a promising class of therapeutics. Centr Eur J Biol 2:1–33

Huang Y, Huang J, Chen Y (2010) Alpha-helical cationic antimicrobial peptides: relationships of structure and function. Protein Cell 1:143–152

Jiang Z, Vasil AI, Hale JD, Hancock REW, Vasil ML, Hodges RS (2008) Effect of net charge and the number of positively charged residues on the biological activity of amphipathic α-helical cationic antimicrobial peptides. Biopolymers (Peptide Science) 90:369–383

Jones DT (1999) Protein secondary structure prediction based on position-specific scoring matrices. J Mol Biol 292:195–202

Kawai F, Shoda M, Harashima R, Sadaie Y, Hara H, Matsumoto K (2004) Cardiolipin domains in *Bacillus subtilis* Marburg membranes. J Bacteriol 186:1475–1483

Konno K, Hisada M, Fontana R, Lorenzi CCB, Naoki H, Itagaki Y, Miwa A, Kawai N, Nakata Y, Yasuhara T, Neto JR, de Azevedo WF Jr, Palma MS, Nakajima T (2001) Anoplin, a novel antimicrobial peptide from the venom of the solitary wasp *Anoplius samariensis*. Biochim Biophys Acta 1550:70–80

Konno K, Hisada M, Naoki H, Itagaki Y, Fontana R, Rangel M, Oliveira JS, Cabrera MPS, Neto JR, Hide I, Nakata Y, Yasuhara T, Nakajima T (2006) Eumenitin, a novel antimicrobial peptide from the venom of the solitary eumenine wasp *Eumenes rubronotatus*. Peptides 27:2624–2631

Konno K, Rangel M, Oliveira JS, dos Santos Cabrera MP, Fontana R, Hirata IY, Hide I, Nakata Y, Mori K, Kawano M, Fuchino H, Sekita S, Neto JR (2007) Decoralin, a novel linear cationic α-helical peptide from the venom of the solitary eumenine wasps *Oreumenes decoratus*. Peptides 28:2320–2327

Kuhn-Nentwig L (2003) Antimicrobial and cytolytic peptides of venomous arthropods. Cell Mol Life Sci 60:2651–2668

Labbé-Julié C, Granier C, Albericio F, Defendini M-L, Ceard B, Rochat H, Van Rietschoten J (1991) Binding and toxicity of apamin. Characterization of the active site. Eur J Biochem 196:639–645

Lohner K, Blondele SS (2005) Molecular mechanisms of membrane perturbation by antimicrobial peptides and the use of biophysical studies in the design of novel peptide antibiotics. Comb Chem High T Scr 8:241–256

Lyu PC, Sherman JC, Chen A, Kallenbach NR (1991) α-Helix stabilization by natural and unnatural amino acids with alkyl side chains. Proc Natl Acad Sci USA 88:5317–5320

Monincová L, Slaninová J, Voburka Z, Hovorka O, Fučík V, Borovičková L, Bednárová L, Buděšínský M, Straka J, Čeřovský V (2009) Novel biologically active peptides from the venom of the solitary bee *Macropis fulvipes* (Hymenoptera: Melittidae). In: Slaninová J (ed) Collection symposium series, institute of organic chemistry and biochemistry, vol 11. Academy of Sciences of the Czech Republic, Prague, pp 77–80

Monincová L, Buděšínský M, Slaninová J, Hovorka O, Cvačka J, Voburka Z, Fučík V, Borovičková L, Bednárová L, Straka J, Čeřovský V (2010) Novel antimicrobial peptides from the venom of the eusocial bee *Halictus sexcinctus* (Hymenoptera: Halictidae) and their analogs. Amino Acids 39:763–775

Monincová L, Slaninová J, Fučík V, Hovorka O, Voburka Z, Bednárová L, Maloň P, Štokrová J, Čeřovský V (2012) Lasiocepsin, a novel cyclic antimicrobial peptide from the venom of eusocial bee *Lasioglossum laticeps* (Hymenoptera: Halictidae). Amino Acids 43:751–761

Oyston PCF, Fox MA, Richards SJ, Clark GC (2009) Novel peptide therapeutics for treatment of infections. J Med Microb 58:977–987

Pazderková M, Kočišová E, Pazderka T, Maloň P, Kopecký Jr. V, Monincová L, Čeřovský V, Bednárová L (2012) Antimicrobial peptide from the eusocial bee *Halictus sexcinctus*. Interacting with model membranes. Spectroscopy Int J 27:497–502

Rohl CA, Baldwin RL (1998) Deciphering rules of helix stability in peptides. Methods Enzymol 295:1–26

Shailesh S, Neelam S, Sandeep K, Gupta GD (2009) Liposomes: a review. J Pharm Res 2:1163–1167

Teixeira V, Feio MJ, Bastos M (2012) Role of lipids in the interaction of antimicrobial peptides with membranes. Prog Lipid Res 51:149–177

Terashima H, Kojima S, Homma M (2008) Flagellar motility in bacteria: structure and function of flagellar motor. Int Rew Cell Moll Biol 270:39–85

Toke O (2005) Antimicrobial peptides: new candidates in the fight against bacterial infections. Biopolymers (Peptide Science) 80:717–735

Tossi A, Sandri L, Giangaspero A (2000) Amphipathic, α-helical antimicrobial peptides. Biopolymers (Peptide Science) 55:4–30

Vemuri S, Rhodes CT (1995) Preparation and characterization of liposomes as therapeutic delivery systems: a review. Pharm Acta Helvetica 70:95–111

Wang G, Li X, Wang Z (2009) APD2: the updated antimicrobial peptide database and its application in peptide design. Nucleic Acids Res 37:D933–D937

Whitmore L, Wallace BA (2008) Protein secondary structure analyses from circular dichroism spectroscopy: methods and reference databases. Biopolymers 89:392–400

Wieprecht T, Dathe M, Krause M, Beyermann M, Maloy WL, MacDonnald DL, Bienert M (1997) Modulation of membrane activity of amphipathic, antimicrobial peptides by slight modification of hydrophobic moment. FEBS Lett 417:135–140

Wimley WC, Hristova K (2011) Antimicrobial peptides: successes, challenges and unanswered questions. J Membr Biol 239:27–34

Yeaman MR, Yount NY (2003) Mechanisms of antimicrobial peptide action and resistance. Pharm Rev 55:27–55

Yeung ATY, Gellatly SL, Hancock REW (2011) Multifunctional cationic host defence peptides and their clinical applications. Cell Mol Life Sci 68:2161–2176

Zaiou M (2007) Multifunctional antimicrobial peptides: therapeutic targets in several human diseases. J Mol Med 85:317–329